RSC Advances

PAPER

View Article Online
View Journal | View Issue

CrossMark click for updates

Cite this: *RSC Adv.*, 2015, **5**, 18233

Multiwalled carbon nanotubes noncovalently functionalized by electro-active amphiphilic copolymer micelles for selective dopamine detection†

Xiaoma Fei, Jing Luo, Ren Liu, Jingcheng Liu, Xiaoya Liu and Mingqing Chen*

We have synthesized an electro-active amphiphilic copolymer with carbazole side chains *via* free radical polymerization using 7-(4-vinylbenzyloxy)-4-methyl coumarin and 9-(4-vinylbenzyl)-9*H*-carbazole as the monomers. The copolymer can self-assemble to form micelles (termed EACMs) in aqueous solution and can adsorb onto the surfaces of MWCNTs *via* π–π interactions and thereby cause the efficient dispersion of the MWCNTs in aqueous solution. The coumarin groups in the copolymer undergo UV-induced photo-crosslinking, which further improves the stability of the suspension. Moreover, the electro-active carbazole moieties in the EACMs can undergo electropolymerization to form a conducting network on the MWCNTs that significantly accelerates electron transfer. The EACM/MWCNTs hybrid was applied to the amperometric sensing of dopamine (DA) as a model analyte. After electropolymerization, the electrode exhibited good sensitivity and selectivity toward the determination of dopamine with a 0.2 μM detection limit and a wide linear range. The method described here provides a viable route to water-dispersible and stable carbon nanotubes while preserving their outstanding electrical properties. We presume that the composite described here represents a valuable tool for the construction of electrochemical sensors and electronics.

Received 23rd December 2014
Accepted 2nd February 2015

DOI: 10.1039/c4ra16923a

www.rsc.org/advances

Published on 02 February 2015. Downloaded by Selcuk University on 12/02/2015 05:00:48.

Introduction

Since the discovery of carbon nanotubes (CNTs) in 1991,[1] CNTs have been the subject of intense interest thanks to their outstanding thermal, mechanical and electrical properties, which lead to wide applications in molecular electronics, sensors, field-emission devices, biological systems, solar cells, and high-performance composites.[2–7] However, extended van der Waals interactions between the side walls of CNTs lead to their aggregation into insoluble and unprocessable bundles of different lengths and diameters, which greatly limits their practical utilities in these applications. To improve their solubility and processability, various carbon nanotube surface modification techniques have been developed, including covalent and noncovalent functionalization.[8–11] In recent years, the functionalization of nanotube surfaces by using amphiphilic copolymers has been recognized as one of the most useful approaches to improve the dispersion of CNTs in aqueous media. Ideally, the hydrophobic segments of an amphiphilic copolymer interact with the surface of the nanotube through hydrophobic interactions, whereas the hydrophilic portions are orientated toward the aqueous phase.[12–15]

Although homogeneous stable aqueous dispersions of CNTs have been achieved using amphiphilic copolymers as dispersants, the electrical properties of the CNTs are sacrificed due to the presence of the insulating polymer dispersant, which is detrimental for their applications in electronic or electrochemical devices because the insulating polymers act as interfacial resistors. In many cases, not only the dissolution of CNTs but also the preservation of the optoelectronic properties of the solubilized CNTs is desirable, leading to the development of CNT hybrid materials with novel and enhanced functional properties. Therefore, it is highly imperative to develop new amphiphilic polymers that could efficiently disperse CNTs without sacrificing their outstanding electrical properties.

Carbazole is one of the electro-active units that could electropolymerize to form a large conjugated structure named polycarbazole (PCz). PCz shows good electrochemical and thermal stabilities as well as photorefractive and photoconductive characteristics.[16–18] It has applications in cathode materials,

Key Laboratory of Food Colloids and Biotechnology, Ministry of Education, School of Chemical and Material Engineering, Jiangnan University, Wuxi, Jiangsu 214122, China. E-mail: mq-chen@jiangnan.edu.cn; Fax: +86-510-85917763; Tel: +86-510-85917763

† Electronic supplementary information (ESI) available: The ^{1}H NMR spectra of EAC; FT-IR spectra of EAC; TEM images of EACM; UV-Vis spectra of EACM/MWCNTs; TGA curves of EACM/MWCNTs; increasing ratios of peak currents for 100 μM DA using different EACM/MWCNTs modified GCE; and CV of the EACM/MWCNTs modified GCE in 100 μM DA solution with the electropolymerization of the carbazole moieties are included in the ESI. See DOI: 10.1039/c4ra16923a

Published on 02 February 2015. Downloaded by Selcuk University on 12/02/2015 05:00:48.

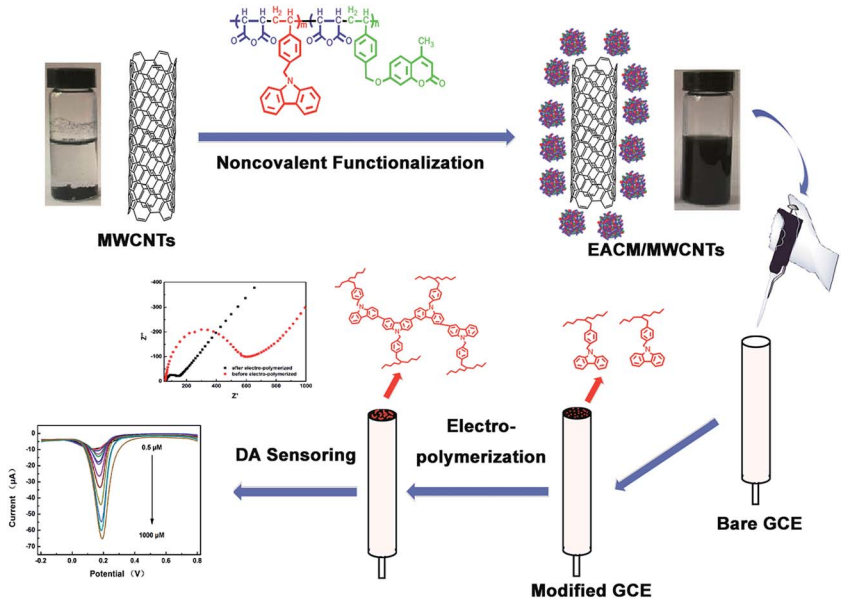

Fig. 1 Scheme of the functionalization of MWCNTs by EACM and the fabrication of a GCE modified by EACM/MWCNTs for dopamine detection.

electrochromic devices and sensors. Several studies have been reported about the incorporation of CNTs into a polymer matrix containing carbazole through chemical and electrochemical methods with the goal of combining the unique properties of CNTs and electro-active carbazole.[19,20] Considering the electroactivity of carbazole and the good electrical conductivity of polycarbazole, it has been questioned whether it is possible to achieve a balance of dispersibility and electrical conductivity for CNTs by using an electro-active amphiphilic copolymer containing carbazole units as a dispersant. On one hand, the amphiphilic copolymer could disperse the CNTs efficiently in aqueous solution; on the other hand, the carbazole unit in the amphiphilic copolymer could electropolymerize to form a conducting network, which could enhance the conductivity and accelerate the electron transfer of the CNT hybrid.

To demonstrate this hypothesis, in this paper, we synthesized a novel electro-active amphiphilic copolymer (EAC) containing carbazole pendants and used its self-assembled micelles (EACM) to disperse MWCNTs in aqueous solution. EACM not only served as an efficient MWCNTs dispersant in aqueous solution but also as a precursor polymer to the formation of a conducting network on the surface of the MWCNTs, which could be formed with the electropolymerization of the carbazole moieties (Fig. 1). The electro-active amphiphilic copolymer was synthesized through free radical copolymerization, and then, it self-assembled into micelles (EACM) in aqueous solution, which could adsorb onto the surfaces of MWCNTs and efficiently disperse the MWCNTs in aqueous solution, resulting in a homogeneous and stable EACM/MWCNTs aqueous dispersion. The coumarin groups of the copolymer chain undergo crosslinking under UV-irradiation, which greatly improves the stability of the obtained MWCNTs suspension. The obtained EACM/MWCNTs dispersion was then casted on an electrode, and the carbazole pendant groups of the EACM underwent electropolymerization by cyclic voltammetry (CV) to form a conducting network on the surfaces of the MWCNTs. Electrochemical impedance spectroscopy (EIS) and CV showed that the electropolymerization of EACM could significantly enhance the electrical conductivity and accelerate the electron transfer of a EACM/MWCNTs hybrid film. Application of the EACM/MWCNTs hybrid in electrochemical sensing was demonstrated by using dopamine as a model analyte. We found that, compared to the non-electropolymerized EACM/MWCNTs, which showed two overlapping peaks of DA and AA, the EACM/MWCNTs after the electropolymerization of the carbazole moieties showed separate peaks of DA and AA with 10-fold higher peak currents in the DPV measurements, indicating enhanced sensitivity and selectivity.

Experimental section

Materials

MWCNTs with a greater than 95% purity were obtained from Timesnano. 2,2-Azobis (isobutyronitrile) (AIBN, Aladdin) was recrystallized twice from ethanol before use. Carbazole (Aladdin), 7-hydroxy-4-methylcoumarin (Acros Organics), 4-vinylbenzyl chloride (Acros Organics), dopamine (DA, Aladdin), ascorbic acid (AA, Aladdin), maleic anhydride (Ma, SCRC), DMF, THF, EtOH, KOH, K_2CO_3, and petroleum ether (60–90 °C, SCRC) were used without further purification.

Characterization

UV-Vis spectra were recorded on a TU-1901 spectrophotometer (Beijing Purkinje, China). Fluorescence spectra were measured on a Cary Eclipse spectrofluorophotometer (Varian, USA). Gel permeation chromatography (GPC) was performed at 35 °C on a Waters-1515 instrument (Waters, USA) with *N*,*N*-

 This journal is © The Royal Society of Chemistry 2015

Published on 02 February 2015. Downloaded by Selcuk University on 12/02/2015 05:00:48.

dimethylformamide (DMF) as the eluent. The molecular weight was estimated by comparison to a polystyrene (PSt) standard curve. Differential scanning calorimetry (DSC) was carried out with a Mettler Toledo DSC822e thermal analyzer. All of the samples were heated at a 10 °C min^{-1} heating rate from 25 °C to 200 °C. The TGA was carried out on a Mettler Toledo TGA/1100SF instrument at a heating rate of 10 °C min^{-1} from 25 ° to 700 °C under a nitrogen atmosphere. The SEM images of each sample of EACM functionalized MWCNTs were taken with a S-4800 field emission scanning electron microscope (Hitachi, Japan). TEM measurements were carried out on a JEOL JEM-2100 microscope operating at 200 kV (JEOL, Japan). Raman spectra were recorded using a Renishaw in Via Raman Microscope (Renishaw, England) operating at 785 nm with a charge-coupled device detector. The cyclic voltammetry (CV), electrochemical impedance spectroscopy (EIS) and differential pulse voltammetry (DPV) were performed using a CHI660E electrochemical workstation (CH Instruments Inc., USA). All of the measurements were conducted at room temperature in a standard three-electrode cell that consists of a glassy carbon electrode as the working electrode, a platinum wire as the counter electrode, and a saturated calomel electrode (SCE) as the reference electrode. The EACM/MWCNTs modified electrodes were prepared by drop-casting certain amounts of the corresponding dispersion on glassy carbon electrodes (dried at 40 °C).

Synthesis of the 7-(4-vinylbenzyloxyl)-4-methylcoumarin (Vm) monomer

The Vm monomer was synthesized according to the literature.[21]

Synthesis of the 9-(4-vinylbenzyl)-9*H*-carbazole (VCz) monomer

Carbazole (7.5 g, 45.0 mmol), potassium hydroxide (4.5 g, 80.0 mmol) and 120 mL of *N*,*N*-dimethylacetamide (DMF) were added to a three-necked flask. After stirring for 15 min, 1-(chloromethyl)-4-vinylbenzene (6.8 g, 45.0 mmol) was added slowly to the mixture, and the reaction was continued for 12 h at room temperature. The mixture was filtered, and the filter cake was washed three times with deionized water to remove the KOH. Afterwards, the filter cake was washed with petroleum ether three times and then dried under vacuum at room temperature for 24 h.

Synthesis of the EAC copolymer

Electro-active amphiphilic copolymer (EAC) was synthesized through free radical copolymerization using Vm, VCz and Ma as monomers. Vm, VCz and Ma were dissolved in DMF at different molar ratios in a round-bottom flask, and then, AIBN was added. The mixture was placed in an oil bath (65 °C) for 24 h under stirring. The resultant copolymers were purified by reprecipitation into EtOH/H_2O (1 : 1 v/v) three times and then were dried under vacuum at room temperature for 24 h.

Preparation of the hybrid of MWCNTs noncovalently functionalized by electro-active copolymer micelles (EACM/MWCNTs)

For the preparation of the stable hybrid of MWCNTs noncovalently functionalized by electro-active copolymer micelles (EACM/MWCNTs), 2 mg of MWCNTs and 5 mg of EAC copolymer were co-dissolved in 1 mL of DMF *via* sonication. Afterwards, the EAC chain was strongly attached to the surfaces of the MWCNTs due to strong π–π interactions. Then, 0.1 mL of deionized water was added dropwise to the solution with strong stirring. During this process, the EAC copolymer self-assembled into micelles on the surfaces of the MWCNTs and further stabilized the MWCNTs. The solution was mildly sonicated and water was added until the volume of DMF : H_2O reached 1 : 9. Then, UV irradiation was carried out with a UV-Vis spot curing system to induce the photo-crosslinking of Vm. After this, there were still some MWCNTs that could not be dispersed. Therefore, the solution was filtered through cotton wool to remove the insoluble MWCNTs, and the obtained filtrate was a photo-crosslinked EACM functionalized MWCNTs dispersion. Finally, the filtrate was dialyzed (molar mass cut off of 14 000) against water to remove DMF and the trace of free copolymer. Due to the strong π–π interactions and photo-crosslinking of EACM around the MWCNTs, the EACM anchored on the MWCNTs is very stable and will not be dialyzed out.

Electrochemical measurements

The EACM/MWCNTs modified electrodes were prepared by dropping certain volumes of the corresponding dispersion on glassy carbon electrodes (GCE) and then drying them at 25 °C. All of the electrochemical measurements were performed using a modified GCE as the working electrode, a platinum wire as the counter electrode, a saturated calomel electrode (SCE) as the reference electrode, and a CHI 660E electrochemical workstation (Shanghai, China). Electropolymerization was carried out in a 0.1 M $LiClO_4$ acetonitrile solution with increasing CV cycles (0–1.5 V, 100 mV s^{-1}). Dopamine detection was carried out in a 0.1 M PBS buffer (pH = 7.0).

Results and discussion

Characterization of the EAC copolymer

Electro-active amphiphilic copolymer (EAC) was synthesized *via* free radical polymerization. Different VCz/Vm feed ratios were used to tune the contents of VCz and Vm in the polymer chain. The structure of the synthetic copolymer was confirmed by ^1H NMR spectroscopy and FTIR. The results were demonstrated in EIS. The basic characterization parameters of the EAC copolymer such as the number average molecular weight (M_n), weight average molecular weight (M_w), molecular weight distribution index (M_w/M_n) and melting temperature (T_m) are given in Table 1.

The maleic anhydride units in the copolymer easily hydrolyze into carboxylic acid in water and thus serve as the hydrophilic segment. The Vm and VCz units function as the hydrophobic segment. Therefore, the obtained EAC copolymer

Published on 02 February 2015. Downloaded by Selcuk University on 12/02/2015 05:00:48.

Table 1 Basic characteristics of the EAC and the EACM/MWCNTs

Sample	n(VCz) : n(Vm) : n(Ma)	M_n	M_w	M_w/M_n	T_m/°C	Polymer content in EACM/MWCNTs[a] (wt%)
EAC0	1 : 0 : 1	8655	9896	1.14	168.9	49.6%
EAC1	1 : 1 : 2	9834	11 420	1.16	164.5	43.4%
EAC2	2 : 1 : 3	8209	9120	1.11	168.3	41.0%
EAC3	3 : 1 : 4	12 703	15 390	1.21	169.1	44.7%

[a] Calculated by TGA.

is an amphiphilic macromolecule and thus can self-assemble into micelles in select solvents. The morphology of the self-assembled copolymer micelles was observed by TEM. As shown in Fig. S3,† the self-assembled micelles were spherical, and their diameters were in the range of 200 to 400 nm.

Characterization of the EACM/MWCNTs dispersion

Four types of EAC copolymers with different amounts of carbazole and coumarin units were prepared by decreasing the feed ratios of Vm as shown in Table 1, and subsequently, they were assembled into micelles (EACM) along with simultaneously functionalizing MWCNTs. The obtained EACM functionalized MWCNTs were named EACM/MWCNTs.

The dispersion efficiency of the MWCNTs in water with EACM was first investigated by visual observation. Pristine MWCNTs and EACM/MWCNTs were sonicated in water for 0.5 h, and the corresponding photographs are shown in Fig. 2a. It can be clearly observed that the pristine MWCNTs completely settled at the bottom of vial within 0.5 h after sonication due to their high surface energy (van der Waals forces). In contrast, all four of the EACM/MWCNTs samples exhibited good dispersibility in water and formed black-colored transparent dispersions. No precipitation was observed after one week of standing.

UV-Vis spectroscopy was used to further investigate the dispersibilities and stabilities of the EACM/MWCNTs aqueous dispersions. None of the EACM/MWCNTs samples exhibited obvious absorption peaks, which was also observed by Rastogi and co-workers.[22] The absorption intensity increased with increasing concentrations of the EACM/MWCNTs dispersion (Fig. S4†), which obeyed Beer's law. These results indicated that the aqueous dispersion of EACM functionalized MWCNTs was homogeneous, and there was no optical behavior typically caused by the aggregation of MWCNTs.

Our previous work has reported that the photo-crosslinking of the copolymer micelles around MWCNTs through the photo-dimerization of the Vm in the polymer chain could encapsulate MWCNTs and further stabilize the noncovalent functionalization.[15] Here, the stabilities of photo-crosslinked EACM/MWCNTs aqueous dispersions with different contents of Vm were studied, and the results are given in Fig. 2b. According to the Beer–Lambert law, the dissolved amount of nanotubes is linearly proportional to the UV absorbance; thus, a higher UV-Vis absorbance means a larger aqueous dispersibility of the functionalized MWCNTs. For MWCNTs functionalized by ECAM0 without Vm moieties, samples with or without photo-crosslinking showed similar dispersibilities and stabilities. The absorbance decreases to approximately 70% of its initial value over a period of two weeks. For MWCNTs functionalized by ECAM1 before photo-crosslinking, the absorbance also decreased with time, and 72% of the initial value was preserved after two weeks. However, after photo-crosslinking, the extent of decrease was much less, and the absorbance remained at almost 90% of its initial value after two weeks. Such results demonstrated that the dispersion stability of ECAM/MWCNTs in water was greatly enhanced by the photo-crosslinking process. The effect of the Vm content in the EAC copolymer on the stability of the ECAM/MWCNTs dispersion was also investigated. As shown in Fig. S5,† EAC1 exhibited best dispersion stability for MWCNTs, which is possibly attributed to the largest amount of Vm in EACM1, which thus leads to the highest degree of photo-crosslinking. So EAC1 was chosen as the original copolymer to investigate the subsequent characterization of EACM/MWCNTs.

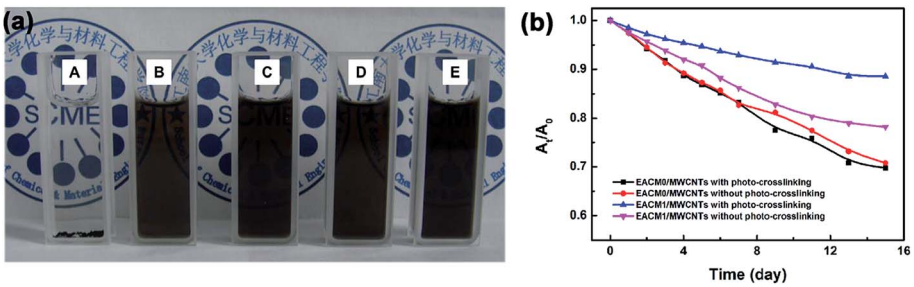

Fig. 2 (a) Photographs of aqueous dispersions of (A) pristine MWCNTs, (B) EACM0/MWCNTs, (C) EACM1/MWCNTs, (D) EACM2/MWCNTs, and (E) EACM3/MWCNTs; (b) the relationship between the stability of the EACM/MWCNTs aqueous solutions and time.

 This journal is © The Royal Society of Chemistry 2015

Published on 02 February 2015. Downloaded by Selcuk University on 12/02/2015 05:00:48.

The surface morphologies of pristine MWCNTs and EACM/MWCNTs hybrids were studied with SEM and TEM techniques. The SEM image (Fig. 3a) exhibits that the pristine MWCNTs were entangled together with a distribution, whereas the image of the EACM/MWCNTs clearly shows that the MWCNTs were tightly covered by a thick layer of copolymers, supporting the functionalization of MWCNTs by EACM. The wrapping of EACM onto the surfaces of MWCNTs was also visualized through TEM images. The image of the pristine MWCNTs (Fig. 3c) shows a smooth surface and agglomerated appearance. In contrast, the image of the EACM/MWCNTs (Fig. 3d) reveals well-separated individual nanotubes, and the MWCNTs' surfaces were wrapped up by copolymer micelles. In addition, hemimicelles and globular micelles could be clearly observed along the MWCNTs just like an untied pearl necklace strung together by MWCNTs. It should be noted that the diameters of the copolymer micelles along the surfaces of MWCNTs were approximately 150 nm, as calculated by TEM. Comparatively, the copolymer micelles without MWCNTs had diameters of approximately 400 nm. Such a difference could be explained as follows: copolymer micelles were formed along the surfaces of the MWCNTs, and thus, their structures and diameters were influenced by the MWCNTs. All of the results described above visually indicated the functionalization of MWCNTs by EACM.

The dispersing mechanism of EACM for MWCNTs in our study may be explained as follows: initially, the EAC copolymer and MWCNTs were co-dissolved in good solvent (DMF) by sonication. Due to the strong π–π interactions between the MWCNTs and the aromatic segments along the EAC copolymer chains, the EAC chains strongly attach to the surfaces of MWCNTs. With the addition of water, the EAC copolymer self-assembles into micelles along the surfaces of the MWCNTs, which results in the stabilization of the MWCNTs in aqueous solution through steric repulsion with a solvophilic hemisphere (Fig. 3d). The presence of interactions between the EAC micelles and MWCNTs was investigated by fluorescence spectroscopy. The fluorescence measurements of the EACM and EACM/MWCNTs were carried out in aqueous solutions by using 295 nm as the excitation wavelength. As shown in Fig. 4, EACM showed strong fluorescence at 445 nm due to the presence of aromatic coumarin and carbazole groups in the polymer chain. In contrast, the dispersion of the EACM/MWCNTs hybrid showed very weak fluorescence emission with the same EACM concentration. By comparing the fluorescence intensities that were determined from the emission peak areas, 96% of the fluorescence emission was quenched in the EACM/MWCNTs with respect to that of EACM, suggesting intramolecular energy and electron transfer between the excited singlet states of coumarin or carbazole moieties and the MWCNTs.[23,24] This significant fluorescence quenching strongly supports an efficient energy transfer from the aromatic moieties to the MWCNTs derived from the π–π stacking interactions *via* vibrational coupling.

Further evidence for existing intermolecular interactions between the EACM and MWCNTs was provided by Raman spectroscopic analysis. The results are shown in Fig. 5. As is known, the graphite G band is related to the tangential mode vibration of the sp^2 C atoms, whereas the D band is induced by scattering from disordered sp^3 C atoms.[25] The ratio of the D-band to G-band of the MWCNTs is a direct indication of the degree of modification of the MWCNTs. In our case, the D

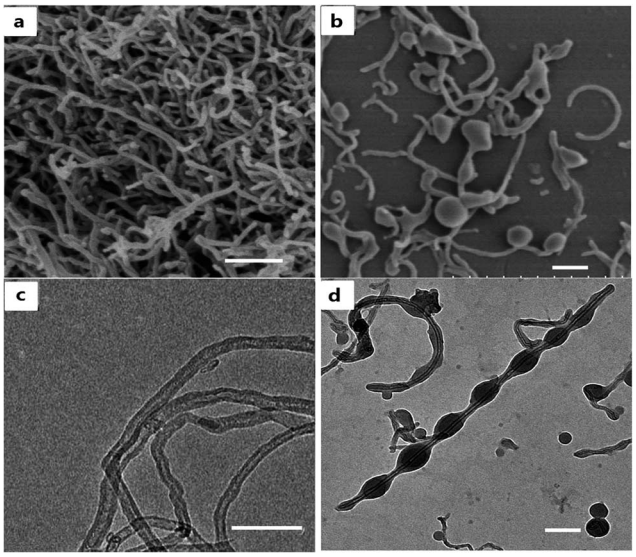

Fig. 3 SEM and TEM images of pristine MWCNTs (a and c), and EACM/MWCNTs (b and d). Scale bar = 200 nm.

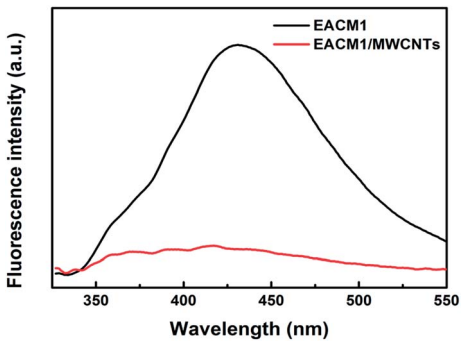

Fig. 4 Fluorescence spectra of EACM and EACM/MWCNTs dispersions in aqueous solutions.

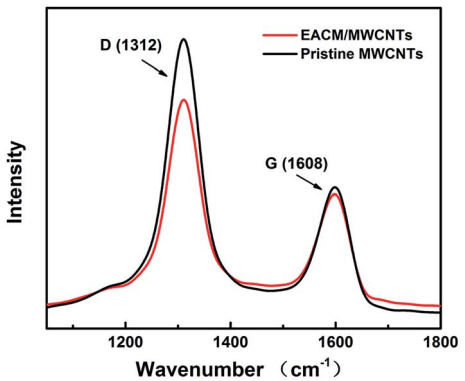

Fig. 5 Raman spectra of pristine MWCNTs and EACM/MWCNTs.

Published on 02 February 2015. Downloaded by Selcuk University on 12/02/2015 05:00:48.

bands and G bands of the EACM/MWCNTs hybrids were observed at 1312 cm^{-1} and 1608 cm^{-1}, respectively. The four EACM/MWCNTs hybrids showed almost the same Raman spectra as pristine MWCNTs. This observation confirmed the noncovalent functionalization of EACM onto the MWCNTs, and it also confirmed that the functionalization process did not lead to any damage to the MWCNTs' structure. Whereas, the slight decreases of the I_D/I_G values of the EACM/MWCNTs hybrids were probably because of the extra sp^2 atom from the π-conjugation of the EACM. Overall, our data suggest adequately strong and stable π–π stacking interactions between the EACM and MWCNTs.

Electropolymerization study

Carbazole is one of the electro-active units that could electropolymerize to form a large conjugated structure named polycarbazole (PCz).[26,27] With the introduction of carbazole moieties into polymer chains and further electropolymerization, a π-conjugated conductive network was formed and thus enhanced the electrical properties of the EACM/MWCNTs. The electropolymerization of the carbazole moieties was executed by employing the CV technique, and the result is given in Fig. 6. An obvious oxidation peak at approximately 1.1 V was observed in the voltammogram, suggesting the formation of a carbazolylium radical cation, which allowed the subsequent electropolymerization of the carbazole units *via* 3,6 connectivity.

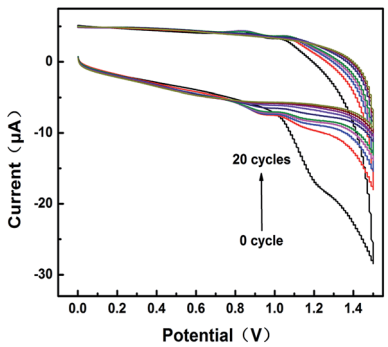

Fig. 6 CV for the electropolymerization of EACM/MWCNTs in 0.1 M $LiClO_4$/ACN at 100 mV s^{-1}.

Electrochemical impedance spectroscopy (EIS) is a well-known and powerful technique for determining the interfacial charge-transfer of films and thus providing direct evidence of electropolymerization. The impedance spectra of EACM/MWCNTs before and after electropolymerization were recorded and are shown in Fig. 7a. The EIS curves are composed of a semicircle region at higher frequencies and a straight line at lower frequencies. The semicircle region corresponds to the electron transfer limited process, and the diameter is equivalent to the electron transfer resistance, which normally reflects the conductivity and the electron transfer process. A GCE modified by EACM/MWCNTs before electropolymerization exhibited a semicircle with a diameter of approximately 620 Ω at the lower frequency region, which is higher than that of MWCNTs (560 Ω). The larger diameter of the EACM/MWCNTs means a higher resistance towards the electron transfer process at the electrode surface, which should be attributed to the presence of the insulating EAC on the MWCNTs. In contrast, after electropolymerization, the modified GCE exhibited a much smaller semicircle region with a diameter of approximately 95 Ω, which indicated the formation of a conducting network through the electropolymerization of carbazole moieties, thus enhancing the conductivity and accelerating the electron transfer of the EACM/MWCNTs. The enhanced electron transfer was also confirmed by CV (Fig. 7b). It was obvious that the anodic and cathodic peak currents of $[Fe(CN)_6]^{3-/4-}$ on the GCE modified by EACM/MWCNTs after electropolymerization were much larger than those of the electrode before electropolymerization. In addition, the potential separation of the redox peaks also became narrower after electropolymerization, indicating faster electronic transport. Both the EIS and CV measurements demonstrate that the electropolymerization of the carbazole enhanced the current response and accelerated the electron transfer of the EACM/MWCNTs.

DA detection

As is known, DA is one of the most important neurotransmitters across all animals, including humans. Alterations in DA contribute to the development of a number of severe mental illnesses, such as Parkinson's disease, schizophrenia and depression.[28,29] Ascorbic acid (AA) has been one of the major

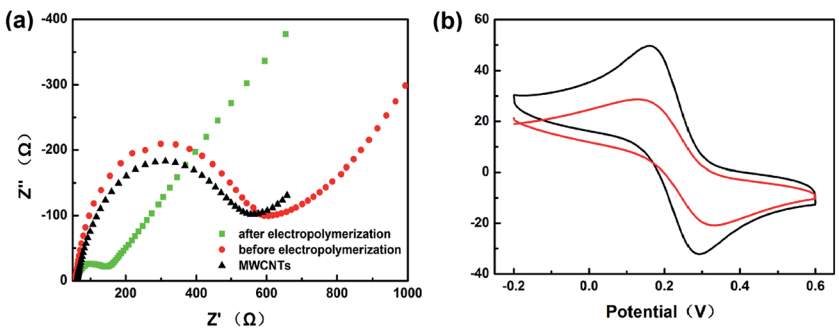

Fig. 7 (a) Nyquist diagrams in 5.0 mM $[Fe(CN)_6]^{3-/4-}$ containing 0.1 M KCl recorded at a MWCNTs and EACM/MWCNTs modified GCE before and after electropolymerization; (b) CV of the EACM/MWCNTs modified GCE before (red) and after (black) electropolymerization in 5.0 mM $[Fe(CN)_6]^{3-/4-}$ containing 0.1 M KCl.

 This journal is © The Royal Society of Chemistry 2015

Published on 02 February 2015. Downloaded by Selcuk University on 12/02/2015 05:00:48.

interfering species due to its abundance in serum samples and its close E_{ox} to that of DA.[30] Therefore, the electrochemical detection of DA in the presence of AA is of great importance. The electrocatalytical ability of a GCE modified by EACM/MWCNTs toward DA is investigated here. As shown in Fig. 8a, compared to the EACM/MWCNTs modified GCE before carbazole electropolymerization, which showed a very small peak current even when the DA concentration was as high as 1000 μM, about a ten-fold higher current response was obtained using the same electrode after the electropolymerization of the carbazole moieties. Such a result suggested that the electropolymerization of carbazole could greatly enhance the electrocatalytical ability of the EACM/MWCNTs, which should be attributed to the increased electrical conductivity and accelerated electron transfer across the EACM/MWCNTs hybrid. In addition, before the carbazole moieties were electropolymerized, the peaks of DA and AA in the DPV measurement overlapped approximately 0.214 V. In contrast, after electropolymerization, the current peak of AA in the DPV measurement shifted to −0.02 V, and the peak of DA barely shifted to 0.192 V, suggesting separation of the peaks of DA and AA. This separation made it possible for the EACM/MWCNTs modified GCE after electropolymerization to detect DA in the presence of AA, suggesting an enhanced selectivity for the modified electrode.

To further realize the contribution of each component in the EACM/MWCNTs to such a good sensitivity and selectivity for the detection of DA, the response of DA on a MWCNTs modified electrode and an EAC1 modified electrode were investigated as control experiments. The results are given in Fig. 9. Compared to the bare GCE, the MWCNTs modified GCE showed a relatively higher electrochemical response toward DA, which can be attributed to the good electrical conductivity of MWCNTs. However, the peak of AA nearly overlaps with that of DA on the MWCNTs modified GCE, indicating a very poor selectivity toward DA and AA. The electrocatalytical ability of an EAC1 modified GCE was also investigated. The EAC1 modified electrode showed a much smaller peak current of DA compared to the bare electrode, which is reasonable considering the insulating property of EAC1. After electropolymerization, the peak current of DA increased significantly, indicating the formation of a conductive network on the GCE. In addition, neither of the peak currents of DA on the MWCNTs (44 μA) or electropolymerized EAC (18 μA) modified electrodes can reach as high as that of the EACM/MWCNTs modified GCE after electropolymerization (67 μA), indicating that the MWCNTs and the conducting EAC network cooperatively contribute to the great response of EACM/MWCNTs toward DA.

The influence of the carbazole content in different EACs on the enhancement ratio of the current response of the corresponding EACM/MWCNTs modified GCE toward DA in DPV measurements was investigated, and the results are given in Fig. S8.† It is clearly observed that among the four EACM/MWCNTs samples, ECAM3/MWCNTs showed the highest enhancement ratio of the current response, which is in accordance with the highest content of carbazole in the ECAM3/MWCNTs. Therefore, the subsequent detection performance

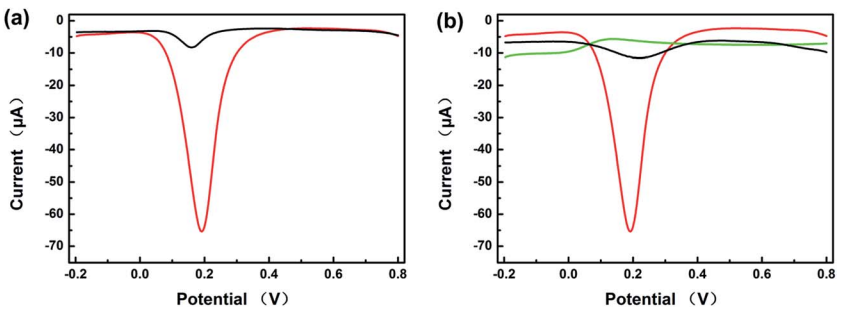

Fig. 8 (a) DPV of 1000 μM DA on a EACM/MWCNTs modified GCE after (red) and before (black) the electropolymerization of the carbazole moieties; (b) DPV of 1000 μM DA in the presence of 1000 μM AA on a EACM/MWCNTs modified GCE before electropolymerization (black) and DPV of 1000 μM DA (red) and AA (green) after electropolymerization.

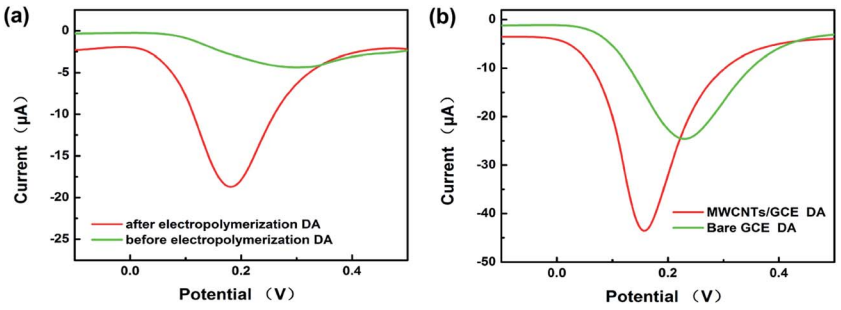

Fig. 9 (a) DPV of 1000 μM DA on an EACM1 modified GCE before (green) and after (red) electropolymerization; (b) DPV of 1000 μM DA on a bare GCE and on a MWCNTs modified GCE.

Published on 02 February 2015. Downloaded by Selcuk University on 12/02/2015 05:00:48.

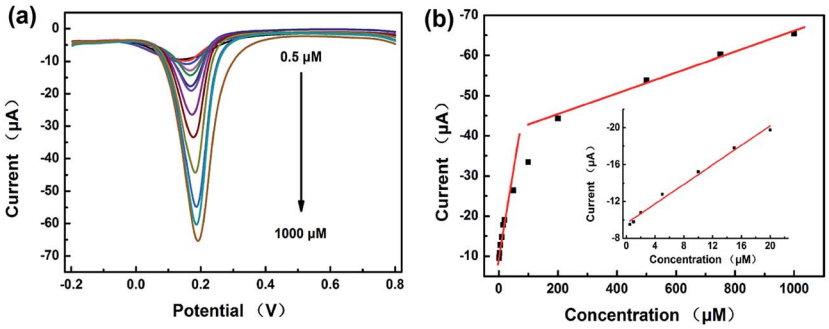

Fig. 10 (a) DPV of different concentrations of DA ranging from 0.5 to 1000 μM on the EACM/MWCNTs modified GCE after electropolymerization in PBS (pH = 7.0); (b) calibration plots of the peak current *versus* the concentration of DA from DPV on the EACM/MWCNTs modified GCE after electropolymerization.

Table 2 Comparison of the performance of our EACM/MWCNTs modified GCE sensor with some previously reported electrochemical sensors for DA

Electrode	Detection method	Linear range (μM)	Detection limit (μM)	Reference
GNP/Ch/GCE	DPV	0.2–80	0.12	Wang *et al.*[31]
Ag/CNT-CPE	DPV	0.8–64	0.3	Tashkhouriana *et al.*[32]
HCNTs/GCE	DPV	2.5–105	0.8	Cui *et al.*[33]
LDH/GC	DPV	1–199	0.3	Wang *et al.*[34]
IMWCNT-CPE	DPV	1.9–771.9	0.52	Nasirizadeh *et al.*[35]
Poly(caffeic acid)/GCE	CV	1–40	0.47	Li *et al.*[36]
GNS/NiO/DNA-GC	CP	1–200	2.5	Lv *et al.*[37]
SDS/CPE	DPV	10–196	0.771	Colín-Orozco *et al.*[38]
C–Ni/GCE	DPASV	0.1–18	0.29	Yang *et al.*[39]
EACM/MWCNTs/GCE	DPV	0.5–20, 200–1000	0.2	Present work

toward DA was investigated based on the ECAM3/MWCNTs modified GCE. Fig. 10 shows the DPV curves of various DA concentrations in PBS solutions on the ECAM3/MWCNTs modified GCE after electropolymerization. The peak current increased with increasing DA concentrations, and the calibration curve for DA showed the following two linear segments: the first linear segment increases from 0.5 to 20 μM with a linear regression equation of $I_1 = -0.5287C_{DA} - 9.632$ ($R^2 = 0.989$), and the second linear segment covers from 200 to 1000 μM with a linear regression equation of $I_2 = -0.02615C_{DA} - 40.17$ ($R^2 = 0.973$). The detection limit was as low as 0.2 μM. In contrast, under the same conditions, the response of the non-electropolymerized control electrode showed very low peak currents for all of the DA concentrations within the test range, and the detection limits were 100 μM, which is three orders of magnitude higher than those after electropolymerization. To make a realistic comparison with previous procedures, the characteristics of different electrochemical sensors for DA are summarized in Table 2. It can be seen that the EACM/MWCNTs modified GCE after electropolymerization showed a low detection limit and its linear range was much wider than those from most of the other sensors.[31–39] The comparison confirmed that our EACM/MWCNTs modified GCE was an appropriate platform for the electrochemical sensing of DA. The above results clearly demonstrated a significantly enhanced sensitivity in DA detection using EACM/MWCNTs modified GCE through carbazole electropolymerization.

The stability of the EACM/MWCNTs modified GCE after electropolymerization was examined by investigating its current response to 1000 μM DA over two weeks. The current response decreased by less than 5.3% of its original response for the 1000 μM DA solution, indicating the good stability of this electrode. To check the reproducibility of our sensor, five electrodes were fabricated independently under the same conditions. A 1000 μM DA solution was measured using the five different electrodes and a relative standard deviation (RSD) of 5.8% was obtained, indicating good reproducibility. These results revealed that the EACM/MWCNTs modified GCE after electropolymerization has a high stability as well as a good reproducibility for the determination of DA, making it applicable for practical use.

Conclusion

In conclusion, a novel amphiphilic copolymer (EAC) with carbazole side chains was synthesized. The obtained copolymer could adsorb onto the surface of MWCNTs *via* π–π interactions and self-assemble into micelles on the surfaces of the MWCNTs, thereby causing the efficient dispersion of the MWCNTs in aqueous solution. The electroactive carbazole moieties could electropolymerize with increasing CV cycles and could form a conductive network on the surfaces of the MWCNTs, which significantly accelerated the electron transfer and enhanced the conductivity of the EACM/MWCNTs. An electrochemical sensor

 This journal is © The Royal Society of Chemistry 2015

Published on 02 February 2015. Downloaded by Selcuk University on 12/02/2015 05:00:48.

for detecting DA was fabricated using an EACM/MWCNTs modified GCE. The results showed that the EACM/MWCNTs hybrid after electropolymerization exhibited a good sensitivity and selectivity with a ten-fold peak current enhancement. This research paves the way for the fabrication of a carbon nanotube/polymer hybrid with high water-dispersibility and stability while preserving their outstanding electrical properties, which would be valuable for the construction of electrochemical sensors and electronics.

Author contributions

The manuscript was written through contributions of all of the authors. All of the authors have given approval to the final version of the manuscript.

Conflict of interest

The authors declare no competing financial interest.

Acknowledgements

We are grateful for the financial support from the National Natural Science Foundation of China (no. 51203063, 21174056), the Fundamental Research Funds for the Central Universities (JUSRP 51305A), and MOE & SAFEA for the 111 Project (B13025).

References

1 S. Iijima, *Nature*, 1991, **354**, 56–58.
2 J. Kong, N. R. Franklin, C. W. Zhou, M. G. Chapline, S. Peng, K. J. Cho and H. J. Dai, *Science*, 2000, **287**, 622–625.
3 R. H. Baughman, A. A. Zakhidov and W. A. de Heer, *Science.*, 2002, **297**, 787–792.
4 A. R. Boccaccini, J. Cho, J. A. Roether, B. J. C. Thomas, E. J. Minay and M. S. P. Shaffer, *Carbon*, 2006, **44**, 3149–3160.
5 W. Jun, C. Yu and J. B. Werner, *J. Mater. Chem.*, 2009, **19**, 7425–7443.
6 C. Zhao, G. Hu, R. Justice, D. W. Schaefer, S. Zhang and M. Yang, *Polymer*, 2005, **46**, 5125–5132.
7 C. Y. Liu and J. M. Hu, *Biosens. Bioelectron.*, 2009, **24**, 2149–2154.
8 V. K. Oxana, I. K. Boris and G. de C. O. Edgar, *RSC Adv.*, 2013, **3**, 24812–24852.
9 Y. L. Liu and W. H. Chen, *Macromolecules*, 2007, **40**, 8881–8886.
10 Z. L. Yao, N. Braidy, G. A. Botton and A. Adronov, *J. Am. Chem. Soc.*, 2003, **125**, 16015–16024.
11 X. Su, Y. Shuai, Z. R. Guo and Y. J. Feng, *Molecules*, 2013, **18**, 4599–4612.
12 H. M. Li, F. Y. Cheng, M. D. Andy and A. Adronov, *J. Am. Chem. Soc.*, 2005, **127**, 14518–14524.
13 Y. Kang and T. A. Taton, *J. Am. Chem. Soc.*, 2003, **125**, 5650–5651.
14 B. Panayiotis, K. Dimitrios, A. Apostolos and S. Georgios, *RSC Adv.*, 2014, **4**, 2911–2934.
15 J. C. Liu, B. Q. Wang, X. M. Xiong, J. Luo and X. Y. Liu, *Chem. Lett.*, 2012, **41**, 50–52.
16 Y. D. Zhang, T. Wada and H. Sasabe, *J. Mater. Chem.*, 1998, **8**, 809–828.
17 J. F. Morin, M. Leclerc, D. Adès and A. Siove, *Macromol. Rapid Commun.*, 2005, **26**, 761–778.
18 T. M. Fulghum, P. Taranekar and R. C. Advncula, *Macromolecules*, 2008, **41**, 5681–5687.
19 M. L. Mayo, D. Hogle, B. Yilmaz, M. E. Köseb and S. Kilina, *RSC Adv.*, 2013, **3**, 20492–20502.
20 S. Lefrant, M. Baibarac and I. Balto, *J. Mater. Chem.*, 2009, **19**, 5690–5704.
21 J. Q. Jiang, Y. Feng, M. H. Wang, X. Y. Liu, S. W. Zhang and M. Q. Chen, *Acta Phys.-Chim. Sin.*, 2008, **24**, 2089–2095.
22 R. Rastogi, R. Kaushal, S. K. Tripathi, A. L. Sharma, I. Kaur and L. M. Bharadwaj, *J. Colloid Interface Sci.*, 2008, **328**, 421–428.
23 H. Paloniemi, T. Ääritalo, T. Laiho, H. Like, N. Kocharova, K. Haapakka, F. Terzi, R. Seeber and J. Lukkari, *J. Phys. Chem. B*, 2005, **109**, 8634–8642.
24 Y. Tomonari, H. Murakami and N. Nakashima, *Chem.–Eur. J.*, 2006, **12**, 4027–4034.
25 M. S. Dresselhaus, G. Dresselhausb, R. Saitoc and A. Joriod, *Phys. Rep.*, 2005, **409**, 47–99.
26 M. Ates and N. Uludag, *Fibers Polym.*, 2010, **11**, 331–337.
27 M. Ates, J. Castillo, A. S. Sarac and W. Schuhmann, *Microchim. Acta*, 2008, **160**, 247–251.
28 K. A. Conway, J. C. Rochet, R. M. Bieganski and P. T. Lansbury, *Science*, 2001, **294**, 1346–1349.
29 B. Rubí and P. Maechler, *Endocrinology*, 2010, **151**, 5570–5581.
30 S. Hou, M. L. Kasner, S. Su, K. Patel and R. Cuellari, *J. Phys. Chem. C*, 2010, **114**, 14915–14921.
31 P. Wang, Y. X. Li, X. Huang and L. Wang, *Talanta*, 2007, **73**, 431–437.
32 J. Tashkhouriana, M. R. Hormozi Nezhadb, J. Khodavesi and S. Javadi, *J. Electroanal. Chem.*, 2009, **633**, 85–91.
33 R. Cui, X. Wang, G. Zhang and C. Wang, *Sens. Actuators, B*, 2012, **161**, 1139–1143.
34 Y. L. Wang, W. Peng, L. Liu and M. Tang, *Microchim. Acta*, 2011, **174**, 41–46.
35 N. Nasirizadeh, Z. Shekari, H. R. Zare and S. Makarem, *Mater. Sci. Eng., C*, 2013, **33**, 1491–1497.
36 N. B. Li, W. Ren and Q. Luo, *J. Solid State Electrochem.*, 2008, **12**, 693–699.
37 W. Lv, F. M. Jin, Q. G. Guo, Q. H. Yang and F. Y. Kang, *Electrochim. Acta*, 2012, **73**, 129–135.
38 E. Colín-Orozco, M. T. Ramírez-Silva, S. Corona-Avendano, M. Romero-Romo and M. Palomar-Pardavé, *Electrochim. Acta*, 2012, **85**, 307–313.
39 S. L. Yang, Y. L. Yin, G. Li, R. Yang, J. J. Li and L. B. Qu, *Sens. Actuators, B*, 2013, **178**, 217.